

# Chapter 1

## A Recurrent Neural Network to Predict G Quadruplex Structure

### Introduction:

Because of the dependence of G4 structure largely on sequence information, it is possible to make predictions about the propensity of specific sequences to form G4s using pattern matching analyses. The initial rule which was employed for putative G4 (PG4) detection in the human genome was the Quadparser method (Huppert & Balasubramanian, 2005). This is a simple regular expression following the pattern  $G_X N_{1-7} G_X N_{1-7} G_X N_{1-7} G_X$  where  $X \geq 3$ . The Quadparser method was chosen based upon early Circular Dichroism and UV melting data, which suggested that G4s tended to be

more stable with three or more tetrads, relatively short loop lengths, and no bulges in tetrads. These fairly stringent rules for formation mean that in general, the Quadparser method is considered to be fairly conservative, and misses a lot of sequences with high G4 forming potential.

More recently there has been a large increase in the number of available methods for predicting G4s (Bedrat et al. 2016, Hon et al. 2017, Garant et al. 2017, Sahakyan et al. 2017). The contribution from Bedrat et al., named G4Hunter, is a scoring method based on a run length encoding the input sequence. Runs of Gs score positively whilst runs of Cs score negatively. It can be used with a sliding window approach to score an entire genome, with thresholding to identify high scoring PG4s. Whilst this approach is much more tolerant of imperfections which violate the Quadparser method, it is arguably too tolerant, producing many false positives. Furthermore, it does not take into account flanking A and T sequences which may contribute to the stability of the G4, e.g. through reducing the favourability of double stranded DNA.

Some middle ground is required to improve existing methods. The current global interest in machine learning for solving biological problems has recently been brought to the field of G4 research, to attempt to solve this issue. The results of this are two new G4 prediction tools, named G4RNA screener (Garant et al. 2017), and Quadron (Sahakyan et al. 2017). The former, G4RNA screener, is a densely connected neural network which is trained on the trinucleotide contents of input sequences. The data used to train the model is a library of melting temperatures of RNA G4s obtained from

a literature search. Currently this database contains only 368 sequences, however. Given the almost inconceivable number of potential G4 forming sequences however (there are more than  $10^{12}$  sequences which could match the original Quadparser pattern, not including flanking sequences), it is probable that this dataset does not capture all of the variety of possible G4 forming sequences. To do this, a more high throughput method for measuring G4 forming propensity is required.

A new method for sequencing of genomic G4 structures, termed G4Seq, may provide this level of throughput (Chambers et al. 2015). To create this dataset, human genomic DNA was sequenced in an Illumina sequencing-by-synthesis machine, in the presence or absence of G4 stabilising potassium cations, or G4 binding ligand Pyridostatin. The G4 structures caused stalling of DNA polymerase, resulting in a large number of errors in the resulting read. Reads were mapped and the mismatch rate which occurred at each position in the genome was then counted to create a map of G4-forming loci. This data was leveraged by Sahakyan et al. to build a gradient boosted machine model, named Quadron, to predict G4 formation. Quadron initially predicts PG4s using the Quadparser method, but with extended loop lengths of 1-12. Various derived features are then extracted from these patterns and used to train a model predicting G4Seq mismatch rate. The primary drawback of this method, is that the Quadparser method is still used to make initial predictions. This means that Quadron is only able to improve the precision of the existing Quadparser method by rejecting false positives that do not form G4s. Since the Quadparser method is already quite conservative, a lot

of potential G4 forming sequences are still missed.

Here we present a new method for G4 prediction, which builds on the work of Bedrat et al. and Sahakyan et al. We use the G4Seq dataset as training data, however a convolutional and recurrent neural network is used to process input sequences directly, meaning fewer prior assumptions are required about what constitutes a G4 forming sequence. Our new method, which we name G4Seeqer, performs better on both the G4Seq datasets and other datasets, including G4s immunoprecipitated from chromatin (Hänsel-Hertsch et al 2016). Finally, we use G4Seeqer to characterise unnoticed features of the G4Seq dataset, and compare our scores to data from UV melting experiments.

## **Materials and Methods:**

### **G4Hunter Algorithm:**

The G4hunter algorithm from Bedrat et al 2016 was reimplemented in Cython (Python superset which can be compiled to C) with some alterations. Input sequences were run length encoded, and each run of Gs was scored as the square of length of the run, with a maximum score per run of 16. These scores were summed to give a positive strand total score. Runs of Cs were scored equivalently but in a separate negative strand score. Scores were divided by the length of the input sequence to get a normalised score.

### **Training Data Preprocessing:**

The modified G4Hunter method was run on the hg19 genome using a window size of 50bp, a step size of 5 and a threshold of 0.75 to generate a total of 7484506 candidate G4 intervals, which were output in bed format. Intervals were increased in size by 39bp in each direction using `bedtools slop` to introduce flanking sequence information for classification. Overlapping intervals were filtered using a dynamic programming technique commonly used in the field of interval scheduling. Intervals were weighted by their G4Hunter score, such that the maximum number of high scoring non-overlapping intervals was yielded.

To ground truth score these sequences, `bedtools map` was used to intersect them with the G4Seq dataset (Chambers et al. 2015), which was downloaded

from GEO (GSEXXXX). Bedgraph files of this data contained percentage mismatch scores for each position of the human genome at 15bp resolution. The G4Seq dataset generated in the presence of potassium was chosen as it was deemed more likely to be of biological relevance than the dataset generated in the presence of Pyridostatin, a G4-binding drug.

Intervals files and corresponding mismatch scores were read into Python using `pandas` and histograms of log transformed mismatch scores were plotted using `matplotlib`. The threshold of approximately 3 for separating G4-forming and non-G4 forming sequences was chosen using `scipy` to determine the local minimum in the histogram. Joint plots of percentage mismatch score against G4Hunter score were plotted using `seaborn`.

Since positive training examples were outweighed in the dataset by a factor of 10:1, random under-sampling of negative examples was conducted using `imbalanced-learn` to attain a ratio of 2:1. This filtered dataset was shuffled and written to disk in bed format, and `bedtools getfasta` was used to extract sequences for each interval from hg19. Sequences were then one hot encoded and loaded into HDF5 format for training using `h5py`. For training of models on trinucleotide content, trinucleotide content statistics were extracted and loaded into HDF5 format.

## Model Training and Validation:

All models were trained in Python using `Keras` with `TensorFlow` backend. The trinucleotide Multi-Layer Perceptron model contained three hidden layers with 16 units per layer. These were trained using the ADAM optimiser

and binary crossentropy loss function, with a dropout rate of 0.2 on all layers. The convolutional portion of G4Seequer was made up of two convolutional layers with 8 filters and kernel size of 3 and ReLu activation, followed by a maximum pooling layer with step size of 2. This was connected to a bidirectional Long Short Term Memory layer with 8 units and Tanh activation. The final hidden layer was a fully connected layer with 16 units, ReLu activation and a dropout rate of 0.5. G4Seequer was trained using the RMSprop optimiser and binary crossentropy loss function.

All models were trained on 80% of the training data with 10% used for validation. Training was done for a maximum of 30 epochs, but with early stopping when the change in validation loss was less than 0.0005 for more than 3 Epochs. The Trinucleotide MLP model converged to this minimum change after 8 Epochs, whilst G4Seequer converged after 15 Epochs.

Models were validated on 10% of the total data held out for testing purposes. Receiver Operator Characteristic (ROC) and Precision Recall (PR) curves were generated using `scikit-learn` and plotted with `matplotlib`. ROC/PR curves for G4Hunter are produced using the modified method. For comparison against Quadron, the Quadron source code was downloaded from GitHub and installed. Since the flanking sequences required for Quadron are longer than those used for G4Seequer, test set sequences were increased in size by 50bp in each direction to 228bp. Sequences were extracted using `bedtools getfasta` and run through Quadron. For intervals which contained multiple Quadron scoring motifs, the highest score was used. For intervals which had no motifs scored by Quadron, a score of zero was assigned.

## **BG4 Analysis:**

NarrowPeak BED files of BG4 ChIP-seq peaks were downloaded from GEO (GSE76688, Hänsel-Hertsch et al 2016). To accomodate Quadron's flanking sequence requirements, the size of the BG4 intervals was increased by 50bp in each direction using `awk`. A BG4-negative peak set was generated using `bedtools shuffle`. Shuffling was done excluding gaps in the genome or BG4-positive peaks. Positive and negative peaks were concatenated and sequences were extracted using `bedtools getfasta`. Predictions were made on these sequences using G4Seequer/G4Hunter/Quadron, and the maximum scoring interval per peak was assigned as the overall score of the peak. Where a model did not make any predictions in a peak, it was assigned a score of zero. Receiver Operator Characteristic (ROC) and Precision Recall (PR) curves were generated using `scikit-learn` and plotted with `matplotlib`.

## **Mutation Mapping analysis:**

Mutation mapping was applied to human promoter regions from the ENSEMBL regulatory build, which was originally generated using ChromHMM. Promoter sequences were extracted from hg38. Mutation mapping was implemented as in Alipanahi et al. 2015: candidate sequences were edited at each position to each nucleotide, and the resulting sequences were scored for G4 formation using G4Seequer. Heatmaps were generated in Python using `seaborn`.

## **G-Triplex and Hairpin analyses:**

G-triplex motifs were predicted in the hg19 genome using an in house script, using the pattern  $G_X N_{1-4} G_X N_{1-4} G_X$  where  $3 \leq X \leq 6$ . Candidate triplexes which overlapped with or were contained within Quadparser motifs (pattern  $G_X N_{1-7} G_X N_{1-7} G_X N_{1-7} G_X$  where  $3 \leq X \leq 6$ ) were subtracted to produce only triplex motifs which could not form “classical” G4s. To assign mismatch scores to these sequences, they were increased in size by 50bp in each direction using `bedtools slop`, and mismatch scores from the G4Seq dataset were mapped using `bedtools map`. Distances to next G-run were measured using Python scripts.

G-hairpin motifs were predicted in the hg19 genome using the same script, and the pattern  $G_X N_{1-4} G_X$  where  $4 \leq X \leq 6$ . Candidate hairpins which overlapped with or were contained within Quadparser motifs or G-triplex motifs were filtered. Intervals were increased in size by 50bp in each direction using `bedtools slop`, and mismatch scores from the G4Seq dataset were mapped using `bedtools map`. Distances to next G-hairpin were measured using `bedtools closest`. Triplex and hairpin histograms and boxplots were generated in Python using `matplotlib` and `seaborn`.

## **Median model score experiments:**

For G4Seeqer scoring of experimentally validated G4s from Guédin et al 2010., sequences were padded using randomly generated sequences to 128bp in length. Left and right padding lengths were also varied at random. 1000

randomly padded sequences were generated and scored per input sequence. Scatter plots of UV melting temperature vs. median G4Seeqer score were produced using `matplotlib`. Errorbars are 68% confidence intervals.

Synthetic sequences used for loop length and G-register experiments were 3 tetrad Quadparser conforming sequences. Each sample contained 5000 randomly generated sequences. Left and right padding sizes and nucleotide contents were varied within random samples. Loop nucleotide contents were also varied. For G-register experiments, the extra G per run was randomly assigned to either the left or right side of the G-run. Loop lengths of 3 were used. Line plots for loop length experiments were generated using `matplotlib`, and errors are 68% confidence intervals. Boxplots were generated using `seaborn`.

### **G-register Experiments:**

For G-register mismatch experiments, 3 tetrad Quadparser conforming G4s from the hg19 genome were identified and the corresponding mismatch score was extracted using `bedtools map`. The number of tetrads with G-register was counted. Boxplots were generated using `seaborn`.

### **Human and Mouse G4 Subpopulation Analyses:**

Example Human and Mouse G4 populations were predicted in hg19 and mm10 using the Quadparser pattern with loop lengths of 3. All possible G4s conforming to this pattern were generated using python `itertools`. Venn diagrams were generated using `matplotlib_venn`. P-values were produced

using hypergeometric tests. Dinucleotide complexity was defined as the total number of unique dinucleotides contained in the motif. Histograms and kernel density estimate plots were produced using `seaborn`. For visualisation of PG4 distributions, a sample of 50000 motifs were randomly selected from the total population of all possible Quadparser motifs with loop lengths of three. These were transformed into two components using UMAP dimensionality reduction, with Hamming distance as the distance metric. Sequences which appear in the human and mouse genome were extracted from the sample. 2D Kernel Density Estimate plots for the full sample, and hg19 and mm10 subsets, were generated using `seaborn`.

# Results and Discussion

## Candidate G4 proposal

One major drawback to any machine learning method for G4 prediction over existing regular expression or pattern based methods is the relative expense of computation. It is therefore not sensible to train and classify a neural network model on all possible input sequences from a genome. Instead we decided to use an existing method, the G4hunter algorithm proposed by Bedrat et al., to produce candidate regions which could then be labelled as true positive G4s or non-G4s, and used as input for model training.

We reimplemented the G4hunter algorithm with some minor modifications. Bedrat et al's method run length encodes the sequence of interest and scored G-runs as the square of the run length, and C-runs as the negative of the square of the run length. These scores are then summed to give an overall score for the sequence. This method was chosen as it was assumed, based on earlier work, that a high G-content on both strands would make the G-Quadruplex unfavourable compared to double stranded DNA. Since we wished to make as few assumptions as possible, and given that the G4seq dataset stems from G4 formation in *in vitro* single stranded DNA, we altered the method to produce two scores. G runs score positively on the positive strand and C runs score positively on the negative strand. This means the sequence d(GGGCCC) would yield a high score on both strands rather than a single score of zero.

To produce candidate regions for model training, we ran the modified

G4hunter method on the human genome (hg19) using a window size of 50bp, a step size of 5bp and a threshold of 0.75. Unstringent values were chosen to produce a high recall, i.e. capture as many true positive G4 structures as possible. These settings produced intervals which overlapped with all PG4 sequences predicted by the Quadparser method using maximum loop lengths of 12. It also produced significantly more sequences that did not conform to the Quadparser method, some of which are likely to form G4 structures.

## Training Data preprocessing

To created training sequences, the 50bp candidate regions from the G4hunter method were increased in size by 39bp in each direction to produce intervals of 128bp in length, since previous work has suggested that flanking regions are an important determinant of G4 stability. Clusters of overlapping intervals were filtered to produce only the interval with the highest G4Hunter score (in cases of ties, a random highest scoring interval was selected). This produced a total of 6237943 candidate intervals. Each candidate interval was then scored by mapping the value of the maximum scoring overlapping window from the G4seq dataset (Chambers et al. 2015), which contains percentage mismatches (%mm) from sequencing in the presence of potassium vs. absence of potassium, in 12bp windows. Regions of high %mm on the positive strand indicate a G4 structure on the negative strand, and vice versa.

Plotting the distribution of the log of the %mm scores produced a bimodal distribution with a peak around 1 (corresponding to 2-3% mismatch) and an-

other around 3.5 (corresponding to approximately 30% mismatch) (Fig. 1.1a). We determined the local minimum in the histogram between the two peaks to be approximately 3 (around 20% mismatch), therefore we used this value to split the data into G4 positive and G4 negative subsets. This yielded more than 10 times more G4 negative sequences than positive, however (5809719 negative to 428224 positive). Since maintaining such an imbalance in the training data would produce a poor classifier, we undersampled the G4 negative class to a ratio of 2:1, yielding a total of 1284672 sequences.

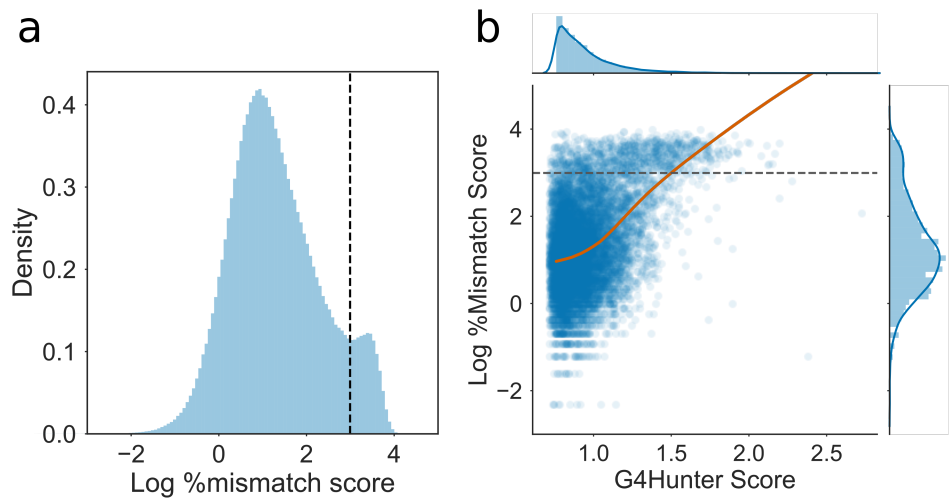


**Figure 1.1: Mismatch scores of candidate sequences identified by G4Hunter:** **a)** Histogram of log percentage mismatch score from the G4Seq dataset, for the 50bp sequences identified by G4Hunter (threshold of 0.75). Dashed line shows the threshold chosen to delimit G4 positive and G4 negative sequences. This corresponded to around 20% mismatch score. **b)** Joint plot of log mismatch score against G4Hunter score for 10000 randomly sampled sequences. Orange line shows lowess curve fit.

## Model selection and training

Previously published G quadruplex prediction methods which utilise machine learning techniques (Quadron, G4RNA) have used derived features such as trinucleotide content to feed to models. These features result in the loss of some spatial information about the sequence, however. For example, the sequence GGTGGTGGTGGGGGG has the same trinucleotide composition as GGCTGGGTGGGTGGG, but is unlikely to have equivalent G4 forming propensity. Furthermore, Quadron derived features require input sequences to conform to the QuadParser regular expression, meaning that Quadron is only able to improve the precision of the QuadParser method, and not the recall. We opted for a neural network involving convolutional layers (those often used for image classification) that could make predictions directly from the sequence itself, without any derived features whatsoever. This allows us to make no assumptions about potential G4 patterns in the dataset. The overall architechture selected was a convolutional-recurrent neural network (Fig. 1.2), which has previously been used to identify regulatory motifs in DNA (DanQ paper). The architechture consists of two one dimensional convolutional layers with a kernel size of 3, to capture local features in the sequence. A maximum pooling layer then reduces the size of the feature space by half. These features are then fed to a bidirectional Long Short Term Memory (LSTM) layer, which is able to learn and recognise long distance relationships between features in the sequence. The model outputs a single value between zero and one of the probability of G4 formation. The dataset was split into three for training and testing: 1332565 sequences (~80%) were

used for training, 166571 (~10%) for in-training model validation, and 166576 (~10%) for post-training model testing.

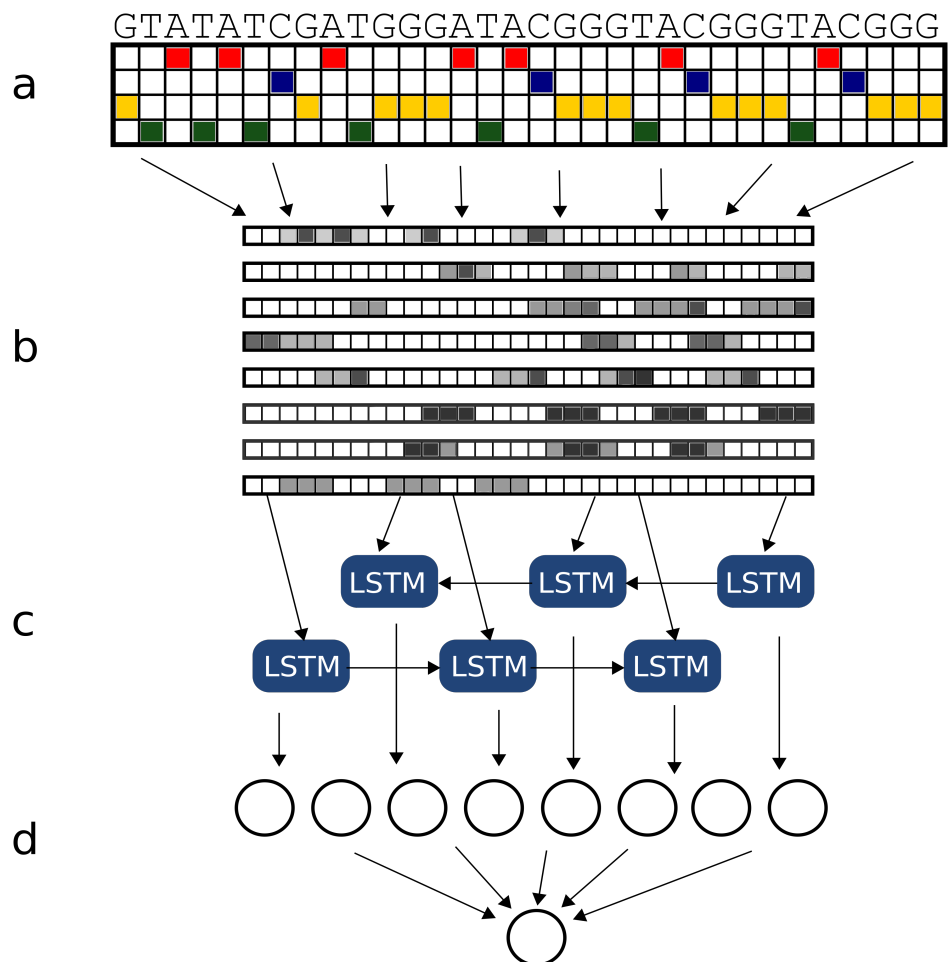


Figure 1.2: **G4Seequer architecture** Adapted from Quang & Xie 2016. **a)** Sequences are one hot encoded to produce a matrix which can be processed by the neural network. **b)** Input matrices are passed through a convolutional layer. Each layer contains 8 filters which are trained to recognise local patterns on the scale of 3-6bp in size. **c)** Convolutional features are passed through a bidirectional Long Short Term Memory (LSTM) layer. This layer recognises long distance interactions between features which might combine to produce G4s. **d)** Finally, features are passed through a fully connected layer. Output from the model is a single probability of whether the sequence forms a G4.

## **Comparison to existing methods:**

We benchmarked our technique (hereafter referred to as G4Seeqr) using the 10% of the data reserved for testing. The model was compared to our modified G4Hunter method, as well as a multi-layer perceptron model trained on trinucleotide frequencies derived from the same dataset as was used to train G4Seeqr. This model allows us to compare the methodology of G4RNA Screener (Garant et al. 2017) to our own method, since G4RNA Screener was originally trained on a database of RNA G Quadruplexes, and may not perform as well on a dataset derived from DNA. The performance of the methods were calculated using the Receiver Operating Characteristic area under curve (ROC AUC). We found that neither G4Hunter nor the G4RNA-like method performed as well as G4Seeqr on the test dataset (AUC G4Hunter 0.82, G4RNA Screener-like 0.90, G4Seeqr 0.94) (Fig. 1.3a-b). This is likely due to the loss of sequence spatial information in the former methods.

To benchmark our method against the other G4Seq trained machine learning G4 prediction package, Quadron, we downloaded and installed the Quadron source code from Sahakyan et al. 2017. Quadron was used to score sequences from the held out test set and compared to the performance of other methods. Quadron requires larger flanking regions of 50bp, so test set intervals and sequences were increased in length by 50bp in both directions to produce test sequences of length 228. This was deemed the best way to compare the two methods, however was still not ideal since Quadron may have been trained on some or all of the test sequences. Regions which had predictions associated with them by G4Hunter and G4Seeqr but had no associated predictions

from Quadron (due to not conforming to the Quadparser regular expression) were given a Quadron score of zero. The ROC curve of Quadron (AUC 0.7) ((Fig. 1.3a-b)) had interesting properties: the model is capable of producing a true positive rate of around 30% with a false positive rate of less than 1%, however shortly beyond this point in the ROC curve the curve becomes linear. This is because Quadron is only capable of scoring sequences which conform to the Quadparser method, with all other sequences being scored zero. Since these sequences only account for a 25% of all the potential PG4 forming sequences in the test set, the model does not perform well on the full dataset. Because it makes no assumptions about the input sequence, G4Seeqer is able to make accurate predictions for all forms of PG4 in the test data, as reflected in the ROC curve.

We were interested in how G4Seeqer compared against Quadron on only sequences which conformed to the Quadparser motif. We therefore filtered our dataset for intervals on which Quadron had made a prediction, and replotted the ROC curves and Precision Recall curves for the filtered data (Fig. 1.3c-d). As expected the AUC for Quadron was much better on this filtered set (AUC 0.93), however it was still outperformed by G4Seeqer (AUC 0.94), suggesting that G4Seeqer captures the same or more explanatory information directly from the input sequence.

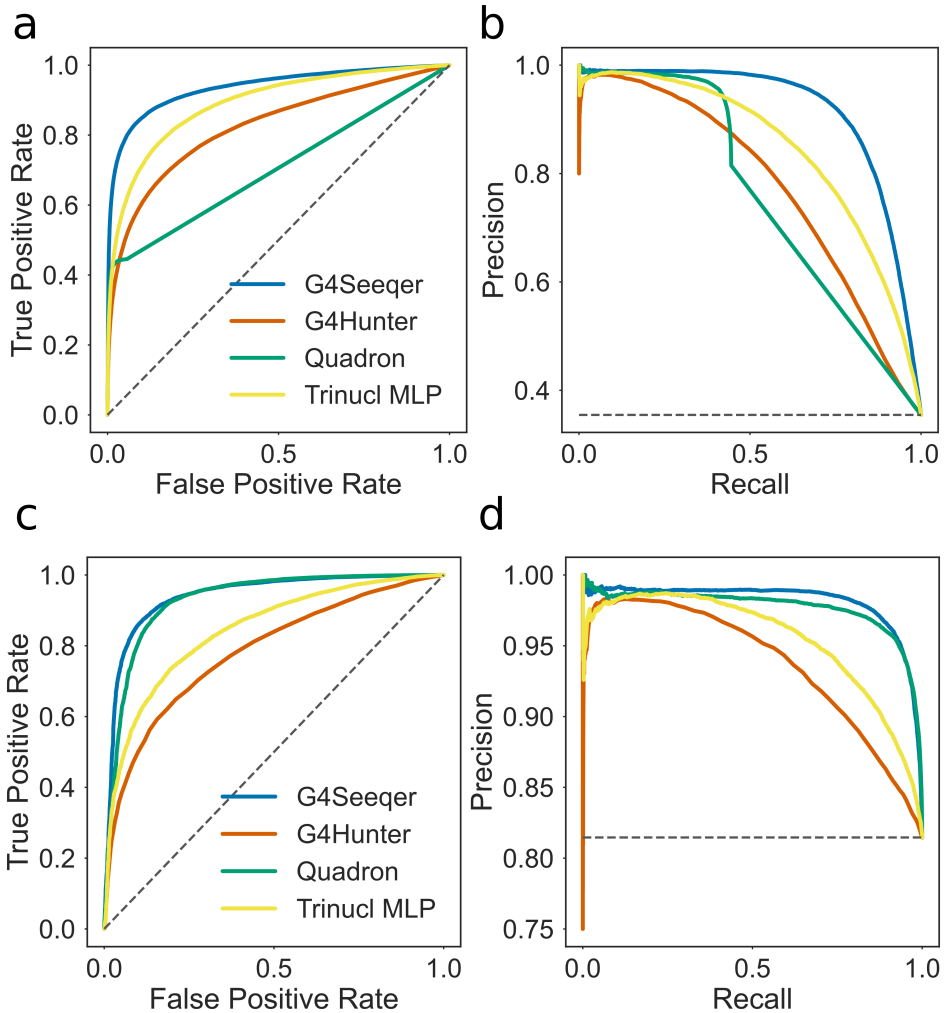


**Figure 1.3: Validation curves for G4Seequer method**

**a)** Receiver Operator Characteristic (ROC) curve showing the performance of G4Seequer, Multi-Layer Perceptron (MLP) trained on trinucleotide contents, Quadron, a Gradient Boosted Machine model (Sahakyan et al. 2017) and the G4Hunter method (Bedrat et al 2016), on a held out test set of the G4Seq dataset (10% of total dataset).

**b)** Precision-recall curves showing the performance of G4Seequer, trinucleotide MLP, Quadron, and G4Hunter on the same dataset.

**c)** ROC curve and **d)** Precision Recall curve showing the performance on sequences from the test set conforming to the Quadparser motif.

## BG4 ChIP-seq data evaluation:

Further model validation was performed on G4s experimentally validated by an entirely different technique, namely G4-chromatin immunoprecipitation (BG4) (Hänsel-Hertsch et al 2016). The BG4 dataset is arguably more biologically relevant than G4seq since G4 structures are not induced by addition of potassium, and are captured from native chromatin. BG4 peak intervals were shuffled to produce a set of G4 negative sequences, and then the performance of the models was evaluated on the real and shuffled peaks. For each BG4 interval, the highest scoring overlapping prediction for each model was assigned. Any intervals with no overlapping predictions were scored zero for that model. We tested the G4Seeqr, G4Hunter and Quadron methods. As with the G4Seq test dataset, we found that Quadron performed reasonably for Quadparser conforming BG4 peaks, but was unable to identify most of the true positive BG4 peaks due to its restriction to the pattern. G4Seeqr performed better on all BG4 peaks, with an AUC of 0.71, however was only marginally better than the G4Hunter technique (AUC 0.7) (Fig. 1.4). These results suggest that the information within the G4Seq dataset, when captured by a suitable model, is predictive of G4s in an *in vivo* setting.

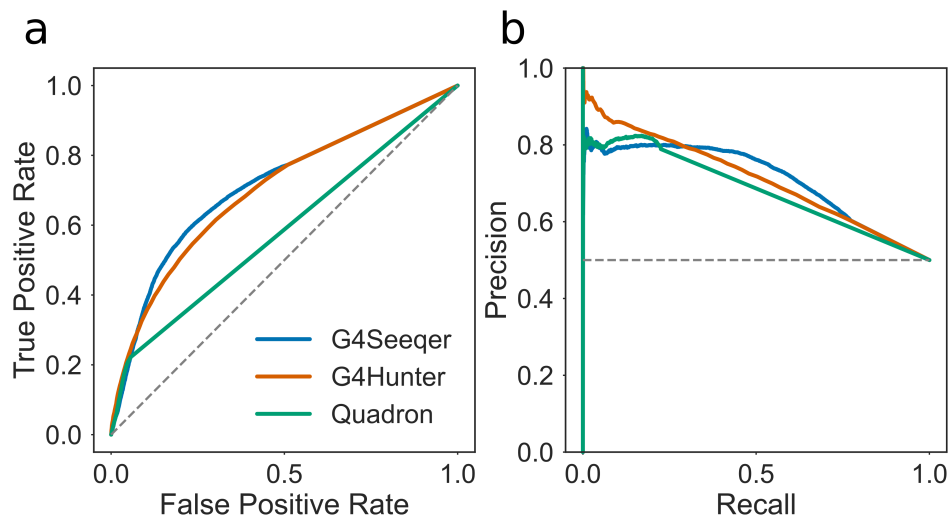


Figure 1.4: **Detection by BG4 peak sequences using G4Seeqer** a) Receiver Operator Characteristic (ROC) curve showing the performance of G4Seeqer, Quadron, and the G4Hunter method, on BG4 ChIP-seq peaks and randomly shuffled negative sequences.

## **Interpreting G4Seequer output using Mutation Mapping:**

One common complaint about machine learning techniques is that the complexity of the models they produce make them “black boxes” which are impossible for humans to understand or extract useful knowledge or rules from. It is possible, however, to visualise some of the output of a neural network through various means. One commonly used method for interpretation is the “saliency” of the network, which can produce heatmaps showing the attention of the network to specific regions of the input image or sequence. This can be used to determine the important aspects of the input in classification. For biological sequences, previous studies have used similar methods, called “Mutation Maps”, to analyse the importance of individual nucleotide positions on CNN model predictions. Simply, the importance of each particular nucleotide is evaluated by replacing it with each of the other three bases, and calculating the change in model score. This is then used to build a heatmap which can be used to visualise the importance of each position.

Previous studies have highlighted a possible role for G4 forming sequences in promoters, with G4 formation tending to have a positive effect on expression, particularly in proto-oncogenes (Eddy & Maizels 2006, Hänsel-Hertsch et al. 2016). We therefore decided to use the mutation map approach to characterise PG4s in promoter regions extracted from the ENSEMBL regulatory build. Promoter sequences were screened using G4Seequer and single base mutation maps were created for each candidate PG4, including those regions where the neural network score was low. Unsurprisingly, all of the most deleterious single base substitutions (causing a score reduction of more

than 0.9) predicted by G4Seeqr mutation mapping were G->H changes.

We identified PG4 sequences scoring more than 0.9 for which a single G->H change resulted in a reduction of as much as 0.9 in score (i.e. switched the score from strongly PG4 positive to strongly PG4 negative) (Fig. 1.5a). Analysis of the mutation maps for these sequences showed that the majority of contained regions containing three G-runs with short connecting loops. These tended to have a long final loop to the next homopolymeric G-run, or no final G-run within the window size. Any G->H mutation in these G-dense regions strongly affected the predicted G4 forming ability. Recent work by Xi et al. has shown that formation of G4 structures in human telomeric sequences occurs via a stable G-triplex structure. We believe these results suggest that the G4seq dataset is either capturing mismatches caused by G-triplex structures, or by G-quadruplexes formed from short range G-triplex interaction with more long range single G-runs. To further illustrate this we predicted all short looped (1-4bp) G-triplexes in the human genome which did not overlap with a Quadparser predicted PG4 (loop lengths 1-12bp). We found that 35% of these were associated with a %mm score greater than 20%, suggesting the formation of some secondary structure (Fig. 1.5b). To see if medium range G-run interactions might stabilise these, we then measured, for each G-triplex, the distance to the next run of at least three Gs on the same strand, and compared this to the %mm score. We found a negative correlation between distance and %mm score (Spearmans rho -0.2) for G triplexes with a G-run less than 100bp away, suggesting that these longer range interactions do occur but become weaker with distance (Fig.

1.5c). This could be due to a reduction in G4 stability with loop length, but could equally be explained by a reduction in the likelihood of the next G-run being contained in the same sequenced fragment. No clear difference was observed in the correlation of %mm score with upstream or downstream G-runs (Spearman's rho -0.17 and -0.15 respectively) suggesting there is no preference for the long loop region to be at the 5' or 3' of the G triplex.

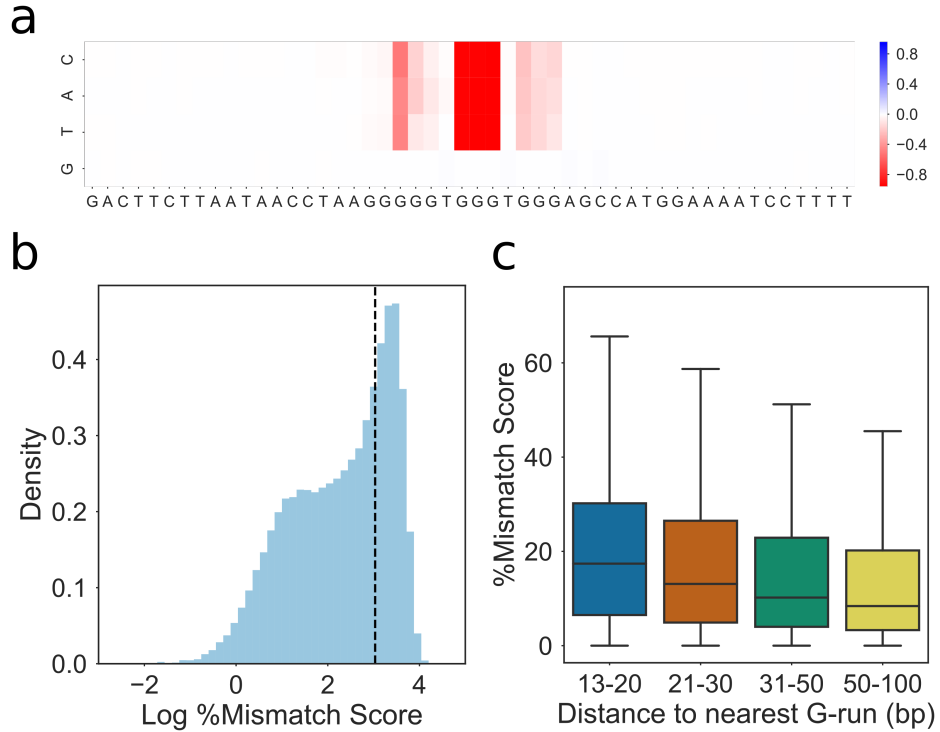


**Figure 1.5: Identification of G-triplex structures by G4Seeqer Mutation Maps**

**a)** Mutation map showing the a high scoring (0.99) G4Seeqer motif which may form a G-triplex. Mutation of any base in the central G-run of the motif is sufficient to reduce the score by up to 80%. **b)** Histogram of log percentage mismatch score for motifs conforming to a G-triplex like pattern. The bimodal distribution suggests that many of these motifs form structures which disrupt polymerase in the presence of potassium. **c)** Box-plot showing the relationship between %mm score and distance to next G-run in G-triplex structures. The negative correlation suggests G-triplexes might recruit distant G-runs to form G4s.

We also noted that G4Seeqr was positively labelling certain sequences which contained only two G-runs, usually of greater than 4 bases in length (Fig. 1.6a). These scores were also very sensitive to G->H mutations. Based on the folding dynamics work by Xi et al, we hypothesised that these sequences might form G-hairpins, which could associate with other nearby hairpins to form G4 structures. To test this, G-hairpins with G-run lengths greater than four were predicted and filtered to remove any overlaps with predicted quadparser G4s (loop length 1-12) or G-triplexes (loop length 1-4). 27% of these sequences had %mm scores greater than 20% (Fig. 1.6b). For each predicted G-hairpin, the distance to the nearest G-hairpin was calculated and correlated with %mm. Again, distance was found to correlate negatively with %mm score (Spearmans rho -0.18), suggesting that these hairpins may associate with each other to form G4s (Fig. 1.6c).

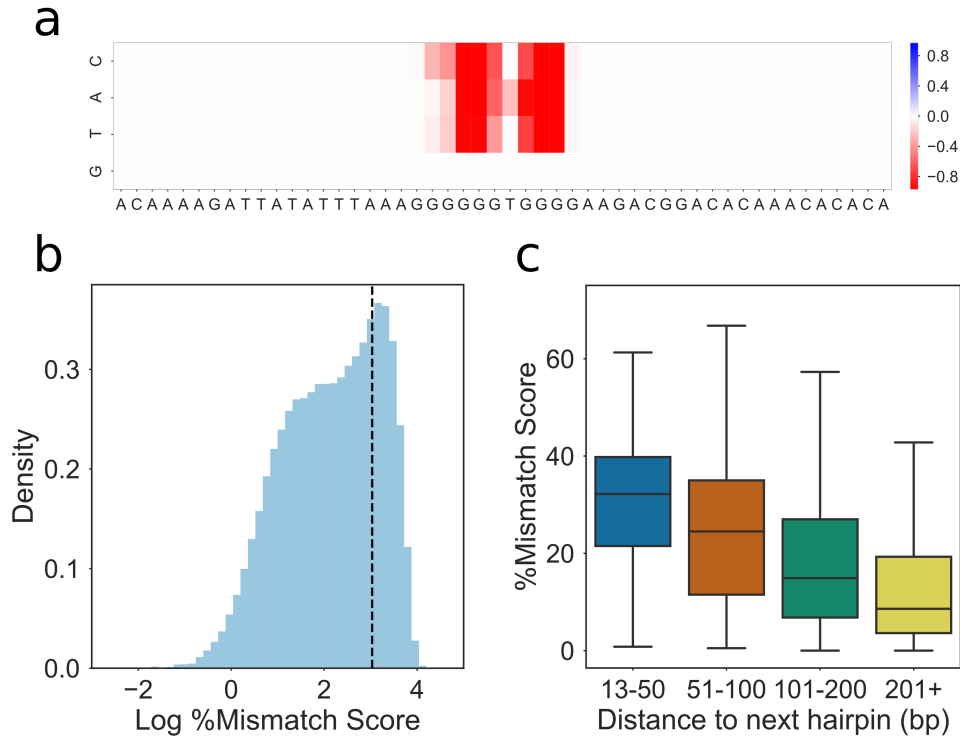


**Figure 1.6: Identification of G-hairpin structures by G4Seeqr Mutation Maps** **a)** Mutation map showing the a high scoring (0.99) G4Seeqr motif which may form a G-hairpin. Mutation of any base in the core motif is sufficient to reduce the score by up to 80%. **b)** Histogram of log percentage mismatch score for motifs conforming to a G-hairpin like pattern. The bi-modal distribution suggests that many of these motifs form structures which disrupt polymerase in the presence of potassium. **c)** Boxplot showing the relationship between %mm score and distance to next G-hairpin for G-hairpin structures. The negative correlation suggests G-hairpins might interact with other relatively distant hairpins to form G4s.

In order to study how interactions between pairs mutations might affect predicted G4 stability, we developed a pairwise mutation map, in which pairs of Gs in each sequence were combinatorially mutated to Ts. We then analysed the resultant mutation maps to identify pairs of G->T transversions which interact to reduce predicted G4 forming potential more strongly than each individual mutation. Perhaps unsurprisingly, we found that in sequences which had more than four G-runs, or had G4s containing features which might form G-triplecs or G-hairpins, mutations which disrupted peripheral G-runs did not have a strong effect on predicted stability. Combinations of mutations which disrupt multiple G-runs had a much stronger effect on stability, however.

## Loop Length and G4 stability.

To determine whether G4Seeqer probability scores supported previous work on the relationship between G4 loop length and stability, we first downloaded UV melting temperatures for three tetrad G4 sequences from Table 1 of Guédin et al. 2010. The majority of these G4 sequences contain only runs of Gs and Ts. In each experiment, one or two of the three T loops were held at a constant length of either 1 or 3, and the other loops varied from 1 up to 15 bp in length. For each sequence, we produced 1000 sequences padded to 128bp (the input length of G4Seeqer) using randomly generated bases, and used G4Seeqer to predict the stability. We found a very strong correlation (Spearman's rho 0.93, p = 1.1e-35) between empirically determined melting temperature in potassium, and G4Seeqer score (Fig. 1.7), suggesting that

G4Seeqr is successfully capturing information about G4 structure which is transferable between conditions. The midpoint of the curve appears to suggest that a melting temperature of around 65oC is required for significant mismatches to occur in the G4Seq dataset. We also noted that G4seeqr output was more variable for sequences with lower melting temperatures, suggesting that sequence context may be more important for these G4s.

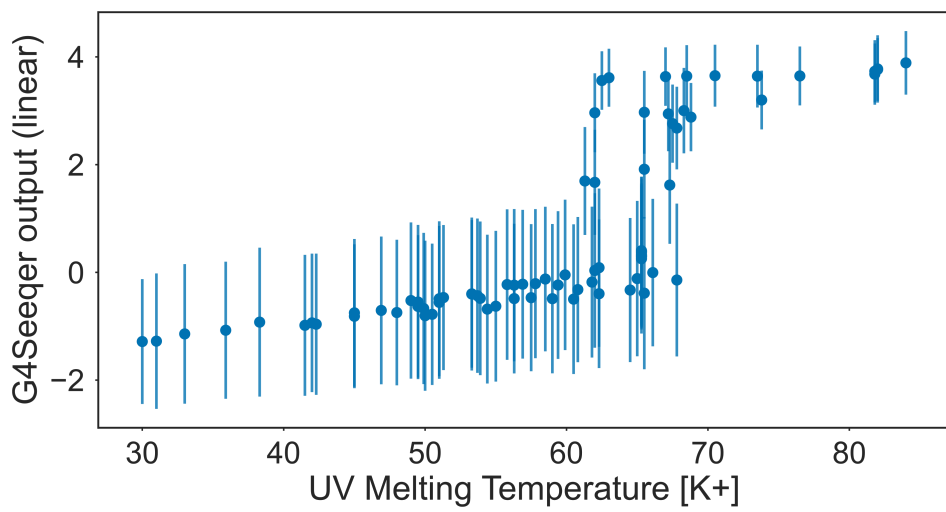


Figure 1.7: **G4Seeqer scores correlate with experimentally determined melting temperatures** Scatter plot showing median G4Seeqer scores vs. UV melting temperature for sequences from Guédin et al. 2010. Error bars are 68% confidence intervals generated from 1000 iterations of prediction with randomly generated flanking sequences.

We next performed a similar *in silico* experiment to that of Guédin et al., whereby we generated random QuadParser conforming G4 sequences with two loop lengths held at 1bp and the third varied from 1-60bp. Loop regions were constructed by randomly selecting from A C or T. The G4Seeqer score for these sequences was then generated. Unsurprisingly, we found that G4Seeqer score reduced with increasing loop length. This effect was strongest for the central loop of the G4, presumably because varying this loop has a greater effect on the ability to form stable G-triplex intermediates (Fig. 1.8a). We then set the length of the non-varying loops to 3bp and re-ran the analysis for third loop length 1-60bp. For these PG4s, we found that the probability of G4 prediction was much more sensitive to longer loop lengths (Fig \ref{loop\\_len}c). There was also no longer a strong difference in prediction when varying the central loop, compared to either loops 1 or 3, possibly suggesting that triplex formation in these sequences is less common.

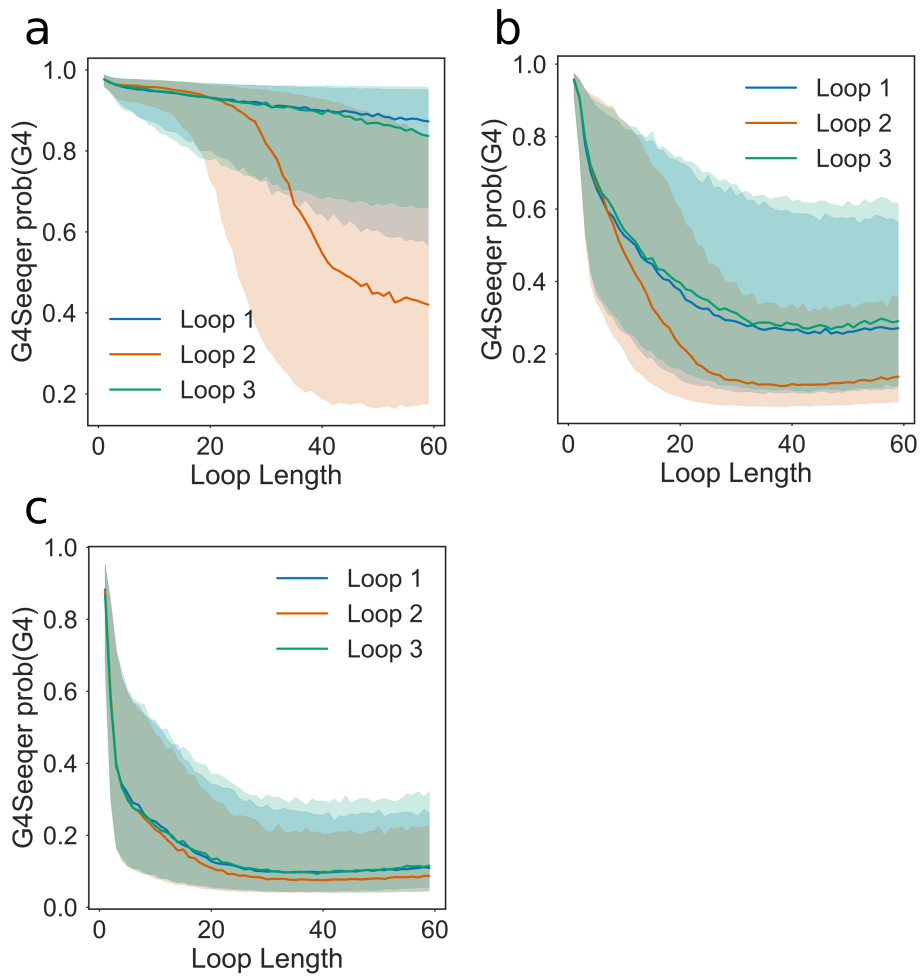


Figure 1.8: **Effect of increasing loop length on G4Seeqer score** **a)** Effect of loop length on predicted G4 stability when other loops are held at a constant length of **a)** 1bp, **b)** 2bp or **c)** 3bp. Median value and 68% confidence intervals are produced using 5000 randomly generated sequences (including flanking regions and loop contents) for each pattern analysed.

## **Effect of G-register on G4 stability.**

Work by Harkness and Mittermaier has indicated that extra Guanines in some G-runs of a G4 forming sequence might increase the G4 forming potential of the sequence, by allowing exchange between different G4 conformations. They termed this effect G-register. We analysed the G4seq dataset and the G4Seequer model outputs to determine whether there was evidence of a relationship between stability and G-register. Firstly, for all PG4s in the human genome conforming to the three tetrad Quadparser motif, we counted the number of G-runs which contained four Gs rather than three. These motifs were then intersected with the G4seq dataset to identify the %mm score. We found that G4seq motifs with greater G-register indeed tend to have higher mismatch scores (Fig. 1.9b). To test whether G4seequer had successfully identified this pattern, we then randomly generated three tetrad PG4 sequences with loop lengths of 3bp, and introduced addition guanines to increase the G-register. Higher G-register strongly increased the G4Seequer score of the sequence, showing that the model has successfully learned this feature of G4s (Fig. 1.9a).

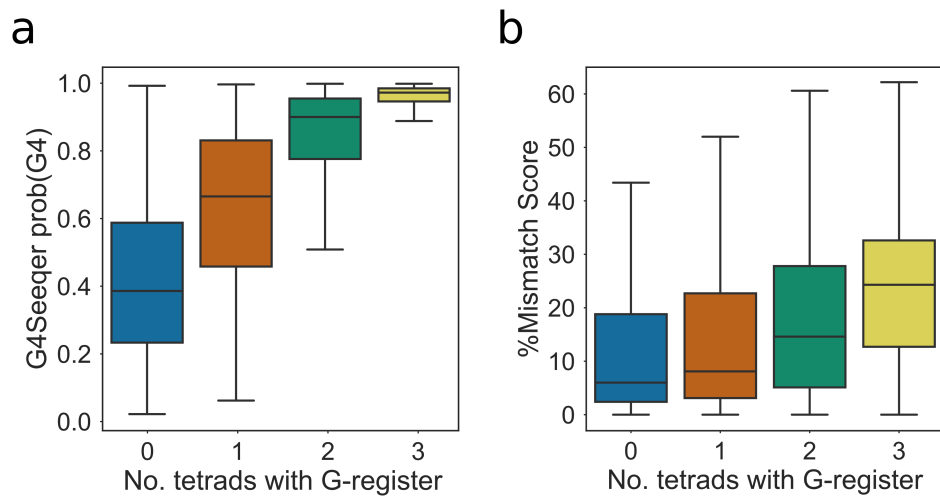


Figure 1.9: **Scoring of G-register effects by G4Seeqer** **a)** Boxplot showing G4Seeqer scores for randomly generated 3 tetrad Quadparser conforming sequences with zero to three additional Guanines per run, referred to by Harkness and Mittermaier as G-register. **b)** Boxplot showing relationship between G-register and %mm score in the G4Seq dataset for Quadparser conforming G4s.

## Applicability of the model to other genomes.

Whilst the Human genome contains a large number of G4 forming sequences, this is not even close to saturating the population of all potential G4s. Indeed, simply considering the Quadparser motif with loop lengths up to 12, there are  $1.1 \times 10^{22}$  different conforming sequences, many orders of magnitude more than there are bases in the human genome. It is probable that the human genome contains a biased subpopulation of all G4s. This might mean that the G4Seeqer model does not generalise well to other genomes which contain different subpopulations. As an example, we analysed 3 tetrad Quadparser motifs from hg19, where all three loops were of length 3. There are  $4^9$  (262144) possible sequences fitting this description, of which only 1.4% (3748) appear in hg19 (Fig. 1.10a). The motifs that did appear tended to be those with lower complexity, as measured by the number of distinct dinucleotides in the sequence, than the total possible population (Fig. 1.10b). The PG4 space of the *M. musculus* genome was also measured, and found to contain 1.7% (4330) of all possible PG4s with loop length 3. There was a strong overlap of 27% ( $p < 2.2\text{e-}308$ ) between sequences in the human and mouse genomes, however, suggesting that at least for this pattern, the PG4 populations of these genomes are comparable. The more complex the PG4 motifs become, however, the more likely it is that these subpopulations will be very different. There are clear differences in dinucleotide content between different genomes, which are often a result of differences in amino acid composition of proteins, or other environmental factors such as temperature. For genomes whose last common ancestor with *Homo sapiens* was longer ago, this divergence

may be much greater. These systemic differences between may result in patterns to which the model has not previously been exposed, and reduce the performance of the model. G4Seeqer, or any other models which are trained on sequences from a single genome, should therefore be used with caution on others.

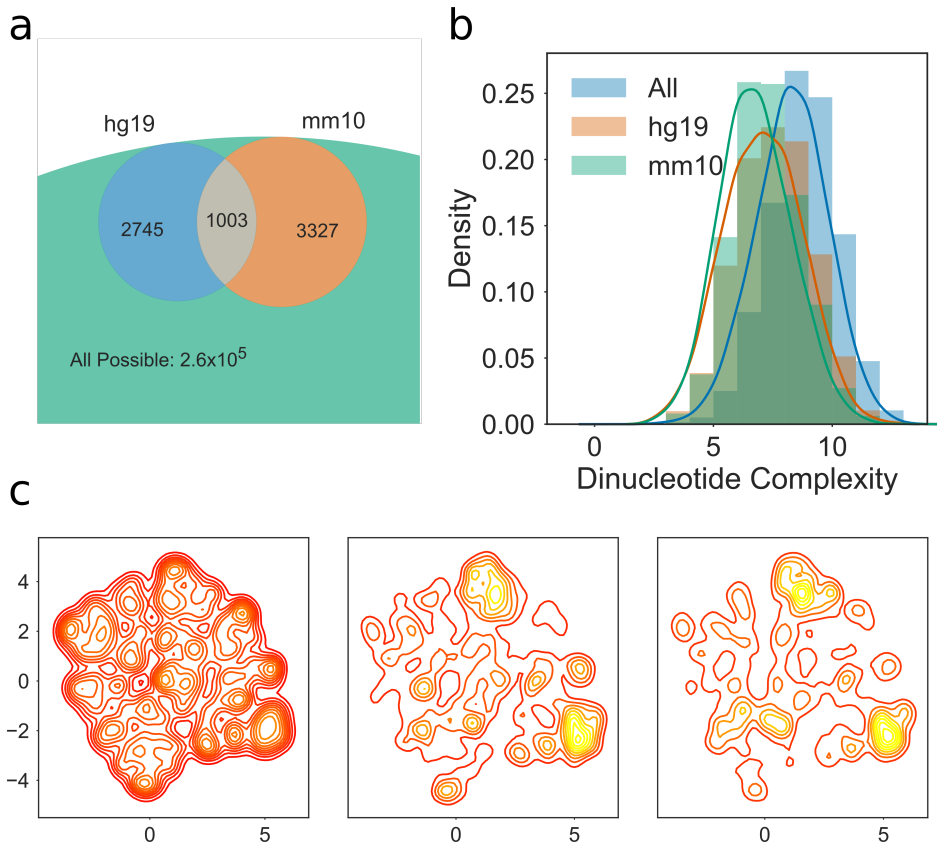


Figure 1.10: **Human and mouse genomes contain different G4 sub-populations** **a)**) Venn diagram showing overlap of 3 tetrad Quadparser motifs populations with loop lengths of 3bp in the human (hg19) and mouse (mm10) genomes, compared to all possible sequences. **b)**) Histogram and kernel density estimate of dinucleotide complexity for human, mouse and all possible 3 tetrad Quadparser motifs with loop length of 3bp. **c)**) 2D Kernel density estimate plot showing distribution of all possible tetrad Quadparser motifs (left), those found in the human genome (centre) and those found in the mouse genome. Dimensionality reduction was conducted using UMAP with Hamming distance as the metric.

## **Conclusion:**

We present G4Seeqr, the first Convolutional/Recurrent Neural Network model for prediction of G Quadruplex forming structures. G4Seeqr is implemented in Python, using Cython for speed-up of G4Hunter candidate region proposal, and Keras with Tensorflow backend for neural network prediction. It is able to process the whole human genome in approximately 1 hour on a 8 core i7 desktop computer with 16GB RAM. Because G4Seeqr is trained directly upon sequences from the human genome, rather than on derived sequence features, it is able to identify patterns in the G4Seq dataset that have not previously been reported, as well as removing false positive sequences which are flagged by pattern matching techniques. This greatly improves the accuracy of the model on various *in vitro* and *in vivo* datasets, from stabilities determined by UV melting to genomic regions identified by BG4 ChIP-seq.